

TWELFTH EUROPEAN ROTORCRAFT FORUM

Paper No. 31

**THE EFFECT OF PITCH RATE ON THE DYNAMIC STALL OF A MODIFIED NACA 23012
AEROFOIL AND COMPARISON WITH THE UNMODIFIED CASE.**

Andrew J. Niven
Roderick A.McD. Galbraith

UNIVERSITY OF GLASGOW

September 22-25, 1986.

Garmisch-Partenkirchen,
Federal Republic of Germany

Deutsche Gesellschaft für Luft- und Raumfahrt e.V. (DGLR)
Godesberger Allee 70, D-5300, Bonn 2, F.R.G.

THE EFFECT OF PITCH RATE ON THE DYNAMIC STALL OF A MODIFIED NACA 23012
AEROFOIL AND COMPARISON WITH THE UNMODIFIED CASE.

Andrew J. Niven, Roderick A.McD. Galbraith,
University of Glasgow.

ABSTRACT

An investigation into the effects of trailing-edge separation on dynamic stall was carried out by modifying and re-testing a NACA 23012 aerofoil. An enhancement in rear separation was obtained by modifying the trailing-edge geometry. To maintain similar flow conditions at the leading-edge, the original aerofoil geometry within this area was left unaltered. The paper presents data obtained from oscillatory and ramp tests and shows the modified aerofoil to have an earlier dynamic stall initiation. It is suggested that this initiation was triggered, at the lower angle of incidence, by the enhanced rear separation.

NOTATION

c	aerofoil chord (m)
C_m	quarter-chord pitching moment
C_n	normal force coefficient
C_p	pressure coefficient
k	reduced frequency ($\omega c/2U$)
k_1	reduced pitch rate ($\alpha \pi c/360U$)
U	free stream velocity (m/sec)
α_b	incidence at which $\Delta C_m = 0.05$
α_c	critical angle of incidence
α_o	zero lift angle
α_{ss}	static stall angle (at C_n collapse)
α	pitch rate (°/sec)
ω	angular frequency (rad/sec)

1. INTRODUCTION

In 1929, the National Advisory Committee for Aeronautics (NACA) began studying the aerodynamic characteristics of a systematic series of aerofoils in an effort to find the shapes that were best suited for specific purposes. Since then, much data has been collected and a fundamental understanding of the dependance of static stall on aerofoil geometry has been obtained (Ref. 1). However, since the advent of the helicopter, a new type of stall became apparent. This characteristic became known as dynamic stall and was a direct result of the highly unsteady conditions found within the rotor flow field. As with the static stall characteristics, a knowledge of the dependance of dynamic stall on aerofoil geometry would be extremely useful.

In recent years there has been significant progress in both theoretical and semi-empirical prediction codes used to model the unsteady effects associated with dynamic stall (a selection of these methods are reviewed in Ref. 2). Clearly, semi-empirical modelling relies heavily on unsteady wind tunnel test data and a knowledge of the factors which effect dynamic stall (Ref. 3). One such factor is the influence of trailing edge separation on the sequential timing of the dynamic stall process.

From the analysis of integrated pressure data, Beddoes (Ref. 3) concluded that, to a first order, there was a common time scale associated with dynamic stall events. The present paper considers the effect of trailing-edge separation on these events by comparing the unsteady performance of two aerofoils which differ only in trailing edge geometry.

2. TEST CONDITIONS

All tests described in this paper were carried out at Glasgow University using an existing rig (Ref. 4) designed to assess the unsteady airloads over an aerofoil undergoing a significant time dependent variance in incidence. Aerofoil performance under static, oscillatory pitch and steady pitch rate (or ramp) conditions can be studied. Chordwise pressure distributions were measured at the mid-span position by 30 transducers mounted within the model. Data acquisition and reduction was carried out by a DEC MINC (PDP 11/23) mini computer (Ref. 5) and during the data processing no account was taken of tunnel blockage or interference effects; these were treated as being unknown.

All the tests were carried out at a Reynolds number of 1.5×10^6 which corresponded to a tunnel Mach number of 0.11.

3. TEST AEROFOIL - A modified NACA 23012 aerofoil

(i) Choice of basic aerofoil

The NACA 23012 represents a typical helicopter rotor profile which utilises the effects of camber to increase its overall aerodynamic performance. For many years this aerofoil has been the subject of intensive testing and the subsequent accumulation of data well documented within the literature. One dominating feature of this profile is its unusual stalling characteristics. On the basis of its abrupt lift collapse one might have expected a leading-edge type stall. However, as predicted by Gault (Ref. 1) this aerofoil should exhibit a trailing-edge stall. This apparent contradiction is due to a rapid growth of trailing-edge separation at a critical angle of incidence.

Using standard experimental techniques (Refs. 6,7), the trailing-edge separation front can be monitored and recorded. As expected, figure 1 shows the NACA 23012 aerofoil to have a rapid forward movement of separation at a critical angle of approximately 14° . For the past few years the NACA 23012 aerofoil has been the subject of exhaustive testing at Glasgow University. This has allowed a reasonable picture of its unsteady stalling characteristics to be obtained and, for this reason, it became the prime candidate for modification.

(ii) Type of modification

A useful modification to the NACA 23012 aerofoil is one which retains the leading edge conditions whilst forcing an earlier and more gradual trailing-edge separation growth.

It is well known (Ref.7) that a region of adverse pressure gradient will, if persistent enough, cause a boundary layer to separate. It follows from this that in order to increase the probability of boundary layer separation, within a given region, one should increase the applied adverse pressure gradient. Therefore, in order to change the separation characteristics of the NACA 23012, a change in adverse pressure gradient over the rear portion should suffice.

A standard vortex panel program (Ref. 8) was used to calculate the inviscid pressure gradient over the NACA 23012 aerofoil (see Figure 2). The upper surface pressure gradient between the 25 and 100% chord position was then increased in severity (Ref. 9) and a new distribution of velocity calculated. An inverse vortex panel program (Ref. 10) was then used to generate an aerofoil possessing this new velocity distribution. This inverse program simply took the "basic" NACA 23012 aerofoil and modified the influence coefficients of the panel matrix to satisfy the new velocity distribution; it was an iterative procedure and, for small modifications in pressure gradient, converged well. The new aerofoil was designated the NACA 23012(A) and is compared to the NACA 23012 aerofoil in Figure 3.

(iii) Verification of modification

To verify that the NACA 23012(A) aerofoil had the desired trailing-edge separation characteristics, a surface oil-film flow visualisation technique (Ref. 6) was used. The static results obtained by this method are shown in Figure 3 where a more persistent and gradual trailing-edge separation may clearly be seen.

4. STATIC PERFORMANCE

Static data was obtained at a Reynolds number of 1.5×10^6 and is presented in Figure 5. The main picture displayed by the NACA 23012(A) aerofoil was the rounding-off in lift-curve slope at a stall angle of 13.6 (0.8° less than the NACA 23012 aerofoil), indicating a trailing-edge type stall. Also observed was a positive pre-stall pitching moment of 0.05; these both being consequences of the reflex trailing-edge.

A further, and interesting, observation that may be made is the obvious non-linearity in pre-stall lift-curve slope. Initial considerations suggested this was a flow phenomenon associated with the reflex trailing-edge; a similar non-linearity is displayed by the GO 738 aerofoil (Ref. 12), at a Reynolds number of 0.5×10^6 , which also has a reflex trailing-edge.

5. OSCILLATORY CHARACTERISTICS

(ii) Overall performance

The variation of C_n and C_m with α is shown in Figure 6 for the two

aerofoils during oscillatory pitch cycles of $10 \pm 8^\circ$ at various reduced frequencies. As expected, both aerofoils displayed the distinctive aerodynamic loadings generally associated with dynamic stall (Ref. 13).

At low reduced frequency (Fig. 7(a)) both aerofoils exhibited similar characteristics, although the NACA 23012(A) displayed a more gradual stall at maximum lift. As the reduced frequency was increased distinct differences between the two aerofoil's characteristics became apparent. Since the two aerofoils had identical nose profiles, it is suggested that these observed differences were due to the influence of trailing-edge separation on the dynamic stall process. These differences, for the 23012(A), may be described as follows :-

- (a) Increased size in C_n and C_m hysteresis (Fig. 6(c)); this is due to the different timing of flow re-attachment during the downstroke.
- (b) Earlier and more gentle C_{ma} break (Fig. 6(b)); this is due to the earlier and more gradual forward movement of the trailing-edge separation front.
- (c) Non-suppression of trailing-edge separation (Fig. 6(d)); the more persistent separation had a slower suppression response to increased reduced frequency. At a reduced frequency of 0.15 the NACA 23012(A) aerofoil clearly exhibited a drop in C_m , at the beginning of the downstroke, which suggested a local increase in rear loading that would accompany a rear separation.

(iii) Critical angle calculation

Following the argument presented by Wilby (Refs. 14,15) a series of oscillatory tests, that took each aerofoil from unstalled to highly stalled conditions, was carried out. This was achieved by keeping both amplitude, $\pm 8^\circ$, and reduced frequency, 0.1, constant whilst varying the mean angle. From the results of these tests, the maximum deviation in C_m , from its pre-stall single loop, was calculated and plotted against the maximum angle of incidence attained in the cycle (see Figure 7). The intercept with the $C_m = 0$ line gives the maximum value of incidence that a given aerofoil can reach before there will be a break in the pitching moment. This angle is known as the critical angle, α_c . For aerofoils intended for use on helicopter rotor blades, it is the difference between the critical angle and the zero-lift incidence, α_0 , that is important. The following data were obtained from static and oscillatory tests :-

NACA 23012(A)	{	$\alpha_0 = 1.0^\circ$ $\alpha_{SS} = 13.6^\circ$ $\alpha_c = 15.6^\circ$	giving $\alpha_c - \alpha_0 = 14.6^\circ$
NACA 23012	{	$\alpha_0 = -1.0^\circ$ $\alpha_{SS} = 14.2^\circ$ $\alpha_c = 16.2^\circ$	giving $\alpha_c - \alpha_0 = 17.2^\circ$

Since the leading-edge pressure distributions of both aerofils are similar, the lower value of α_c exhibited by the NACA 23012(A) aerofoil

must be caused by trailing-edge separation aggravated by the more severe rear pressure gradient. The lower value of α_c , coupled with a higher value of α_o , gives the NACA 23012(A) aerofoil a greatly reduced value of $\alpha_c - \alpha_o$ indicating a poorer performance in the unsteady regime.

6. RAMP CHARACTERISTICS

(i) Overall performance

The dynamic stall rig at Glasgow University provides a useful facility to obtain the aerodynamic characteristics of an aerofoil undergoing a ramp like variation in incidence. These ramp motions are of great value in studying the effects of pitch rate on the sequential timing (Ref. 16) and manner of dynamic stall.

At significant values of pitch rate (i.e. $k_1 > 0.004$) Seto and Galbraith (Ref. 17) observed the stall to acquire certain typical characteristics. These were:

- (a) Large dynamic overshoot of C_n and C_m .
- (b) Vortex shedding (see Figure 8) and subsequent increase in C_n .
- (c) Collapse of C_n and associated development of a large negative pitching moment.

The effect of pitch rate on the upper surface pressure distribution, during the stall process, is illustrated in Figure 8. Figures 9 and 10 show the unsteady lift and pitching moments for the NACA 23012 and 23012(A) aerofoils respectively. Although the overall characteristics are very similar, the NACA 23012(A) exhibits, generally, more gradual variations in lift and pitching moment, especially at the higher pitch rates. It also displays a larger reduction in the unstalled static lift-curve slope and an earlier development of the maximum negative pitching moment.

(ii) Pitching-moment break

In Beddoes' analysis (Ref. 3) he concluded that, during a dynamic increase in incidence, an aerofoil will incur a break in pitching-moment, a period of time, Δt , after passing, and remaining above, its static pitching-moment break incidence. Beddoes gave the value of this time delay as :

$$\Delta t = \frac{nc}{U} \quad \text{where } n = 2.44$$

From the ramp data, collected at Glasgow University, the variation of pitching-moment break with pitch rate was obtained for each aerofoil. Subsequent analysis followed that given by Wilby (Ref. 14), in which a definition of pitching-moment break is taken as the angle of incidence, α_b , for which the value of C_m had fallen by 0.05 below its maximum value. Plotting these values against $\dot{\alpha}/U$ and calculating the resultant slope gives a value for n in the above equation.

It is apparent, from Figure 11, that the variation of α_b , does not possess a unique linear dependance on $\dot{\alpha}/U$ throughout the full range of pitch

rates. However, in conformation with those data obtained by Wilby (Ref. 14), it was inferred that a linear relationship existed for values of less than 2.0. The results from these analyses and their implications are discussed below.

(iii) Sequential timing of dynamic stall

For the NACA 23012(A) aerofoil, a value of 2.5 was obtained for n which is consistent with that given by Beddoes. However, a high value of 3.8 was measured for the NACA 23012. Although the extent to which these time delays are effected by local tunnel conditions is arguable, the important feature of Figure 11 is the different slopes obtained for each aerofoil. The implication then is that, since both aerofoils were tested under similar conditions, the variation in time delay was mainly due to the influence of trailing-edge separation on the onset of dynamic stall.

Figures 12 and 12(b) present, in the manner of Ref. 18, chordal C_p values for both aerofoils undergoing a ramp variation of incidence at a reduced pitch rate of 0.01. These data contained evidence that the two aerofoils exhibited subtle differences in their unsteady stalling characteristics; comparing any two C_p traces clearly demonstrates this. This can cause difficulties when attempting to quantify the sequential timing of events incurred during dynamic stall (Ref. 16).

7. CONCLUSIONS

On the basis of the data and discussions presented, the following conclusions have been drawn.

- (a) Aerofoils displaying a prominent trailing-edge stall under static conditions are likely to exhibit dynamic stall triggered by a rear separation. However, this separation can be suppressed by increasing the pitch rate.
- (b) The exact mechanism by which rear separation effects dynamic stall is, at present, unclear although it does tend to give an aerofoil a poorer unsteady performance.

ACKNOWLEDGEMENTS

The authors wish to express their thanks to Professor Richards for his support and encouragement. Also to P. Wilby (RAE, Farnborough) and T. Beddoes (Westland Helicopters), for their continued help and discussions. The work was carried out in collaboration with Westland Helicopters via an SERC CASE aware No. 8051/3408 and MOD Agreement No. 2048/026 XR/STR.

REFERENCES

1. D.E. Gault A correlation of low-speed airfoil-section stalling characteristics with Reynolds number and airfoil geometry.
NACA TN 3963, 1937.
2. T.S. Beddoes Prediction methods for unsteady separated flows.
Aeromechanics Dept., Westland Helicopters, Yeovil, Somerset.
3. T.S. Beddoes A synthesis of unsteady aerodynamic effects including stall hysteresis.
Aeromechanics Dept., Westland Helicopters, Yeovil, Somerset.
4. G.J. Leishman Contributions to the experimental investigation and analysis of aerofoil dynamic stall.
Ph.D. dissertation, University of Glasgow, Scotland.
5. R.A.McD. Galbraith A microcomputer based test facility for the and
J.G. Leishman investigation of dynamic stall. Paper E3,
International Conference on the Use of the Micro
in Fluid Eng., 1983.
6. L.Y. Seto,
Leishman and
R.A.McD. Galbraith An investigation of three-dimensional stall J.G.
developments on NACA 23012 and NACA 0012 aerofoils.
Glasgow University Aero Report No. 8300, Oct. 1984.
7. P.K. Chang Control of flow separation.
Hemisphere Publishing Corp., Washington, London,
1976.
8. J.G. Leishman and
R.A.McD. Galbraith An algorithm for the calculation of the potential
flow about an arbitrary two-dimensional
aerofoil. Glasgow University Aero Report No.
8092, May 1981.
9. A.J. Niven and
R.A.McD. Galbraith A design procedure to modify the trailing edge
upper surface pressure gradient of a given
aerofoil. Glasgow University Aero Report No.
8408, July 1984.
10. M. Veza and
R.A.McD. Galbraith A comparison of two methods for the design of
aerofoils with specific pressure distributions.
Glasgow University Aero Report No. 8303, June 1983.
11. B. Thwaites Incompressible Aerodynamics.
Cambridge University Press, 1961.
12. S.J. Miley A catalog of low-Reynolds-Number Aerofoil data for
wind-turbine applications. Dept. of Aerospace
Engineering, Texas A&M University, Feb., 1982.

13. T. Beddoes A qualitative discussion of dynamic stall.
Aeromechanics Dept., Westland Helicopters, Yeovil,
Somerset.

14. P.G. Wilby The aerodynamic characteristics of some new RAE
blade sections and their potential influence on
rotor performance. Vertica, Vol. 4, pp 121-133,
1980

15. P.G. Wilby An experimental investigation of the influence of
a range of aerofoil design features on dynamic
stall onset. Tenth European Rotorcraft Forum,
Aug., 1984.

- 16 R.A.McD. Galbraith On the duration of Low Speed Dynamic Stall.
A.J. Niven and 1986 ICAS Conference, London, Sept. 1986.
L.Y. Seto

17. L.Y. Seto and The effect of pitch rate on the dynamic stall of a
R.A.McD. Galbraith. NACA 23012 aerofoil. Eleventh European
Rotorcraft Forum, London, Sept. 1985.

18. W.J. McCroskey, Dynamic stall on advanced airfoil sections.
K.W. McAlister AHS J., Vol. 26, No. 3, 1981.
L.W. Carr and
S.L. Pucci

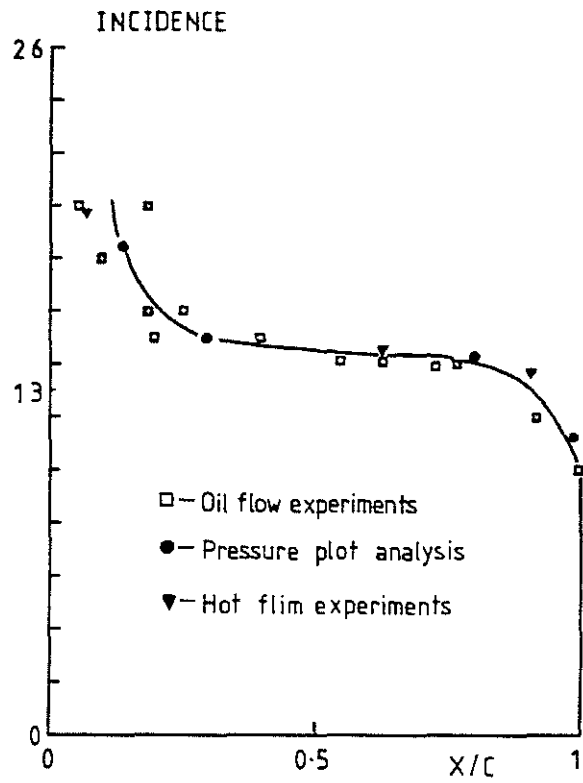


Fig.1 SEPARATION CHARACTERISTICS FOR THE NACA 23012 AEROFOIL

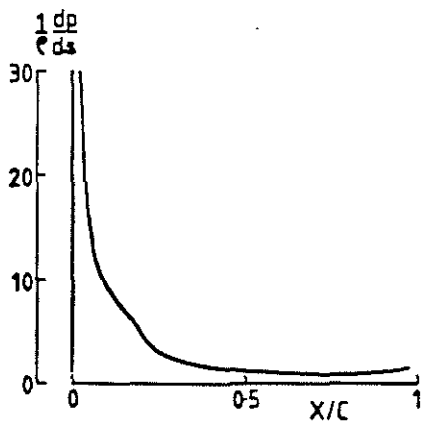


Fig.2 INVISID PRESSURE GRADIENT (NACA 23012)

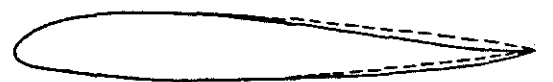
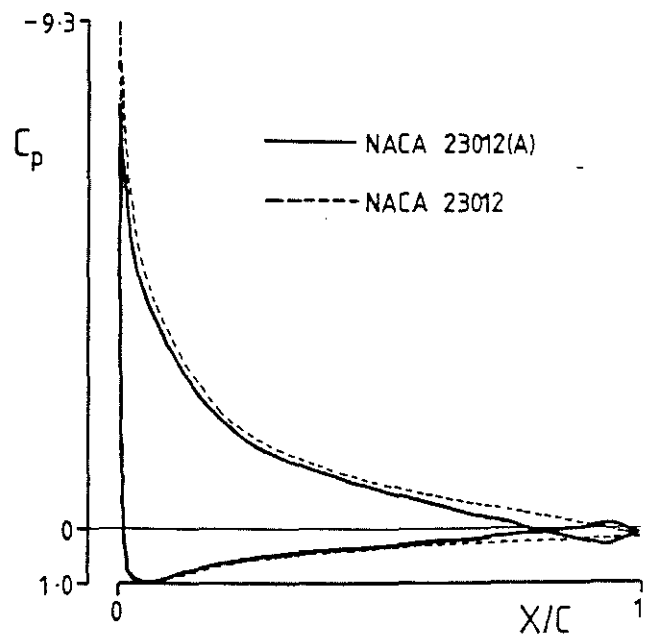


Fig.3 RESULTS FROM AEROFOIL DESIGN PROCEDURE

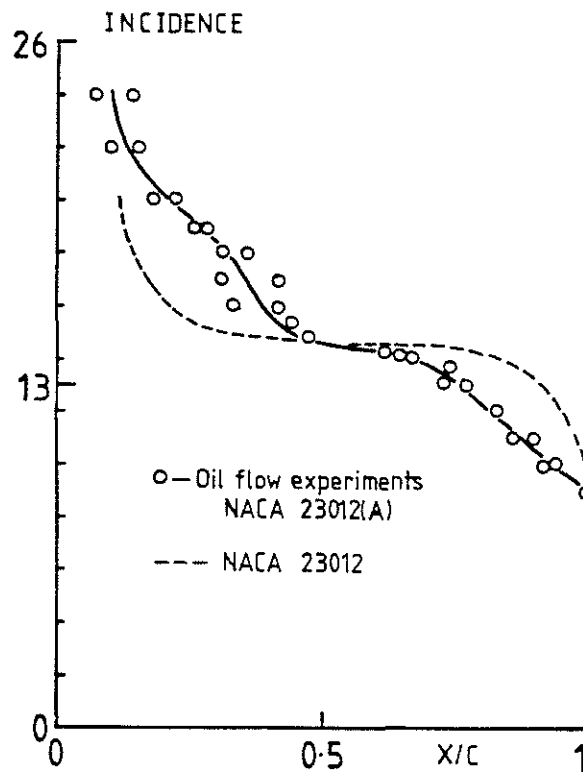


Fig.4 SEPARATION CHARACTERISTICS FOR THE NACA 23012(A) AEROFOIL

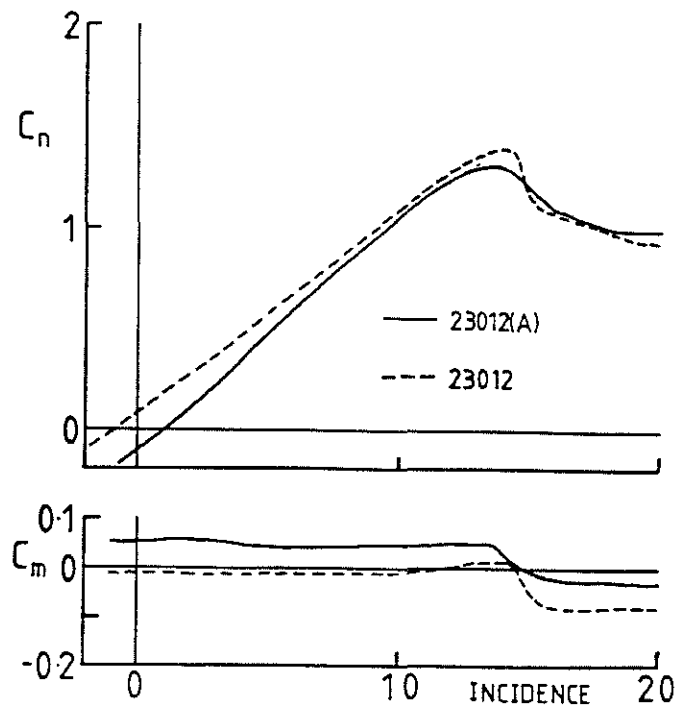


Fig.5 WIND TUNNEL CHARACTERISTICS (STATIC DATA)

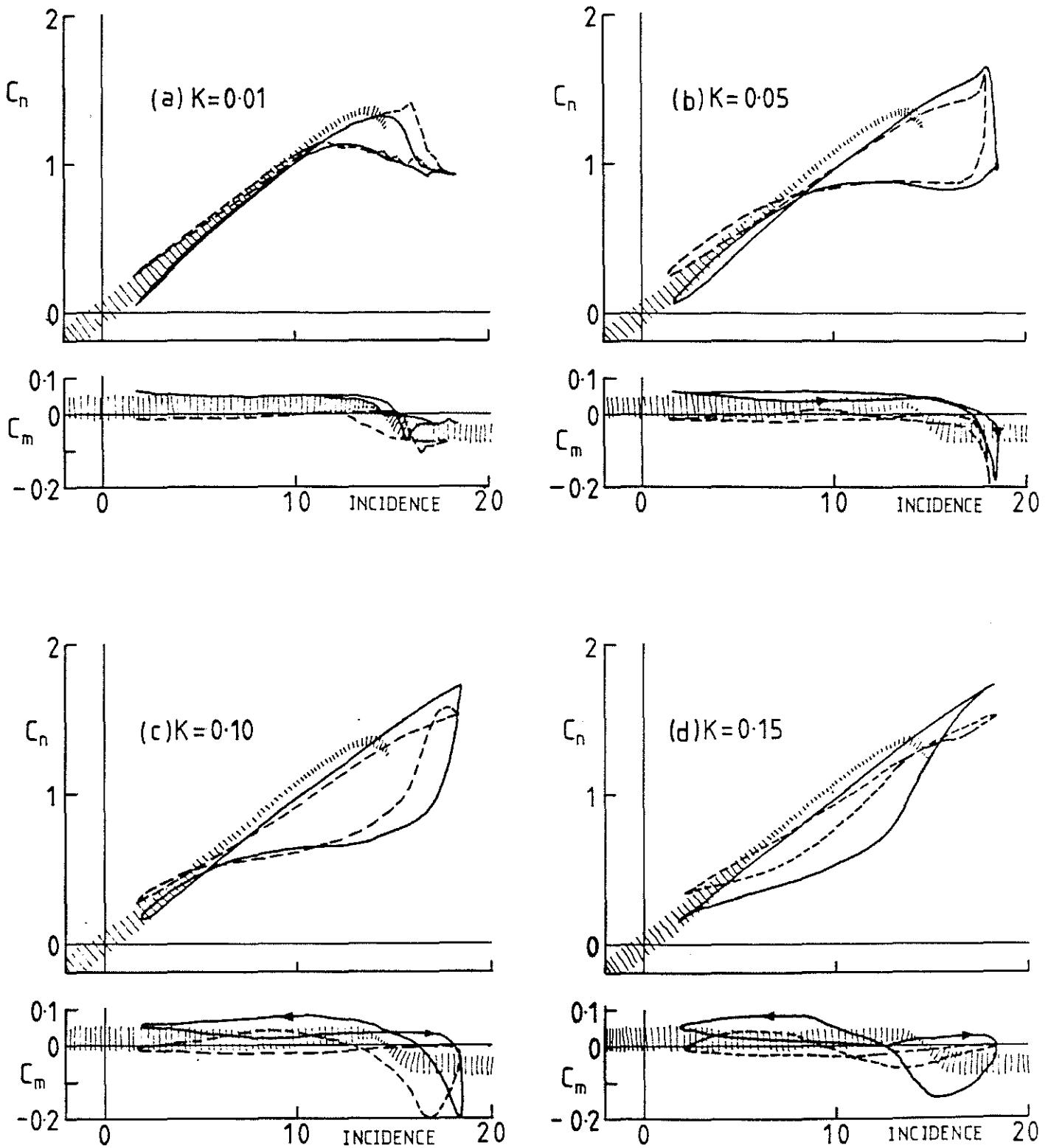


Fig.6 PERFORMANCE DURING OSCILLATORY TESTS

Note: — NACA 23012(A)
 - - - NACA 23012
 ▨ Combined Static Test Results
 of both Aerofoils

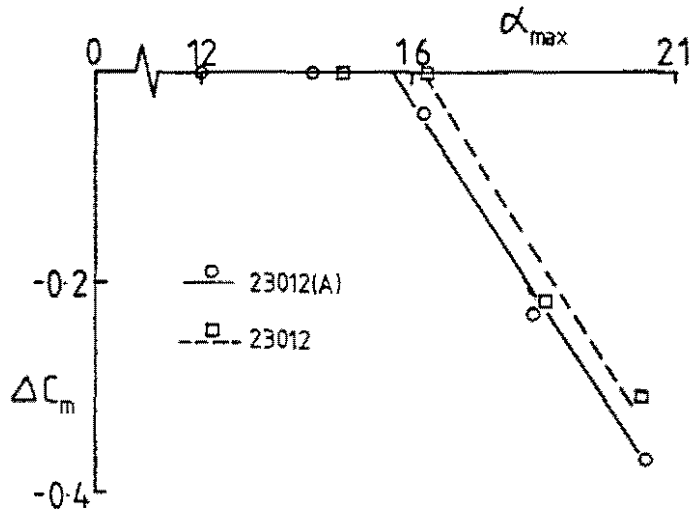


Fig. 7 CRITICAL ANGLE CALCULATION

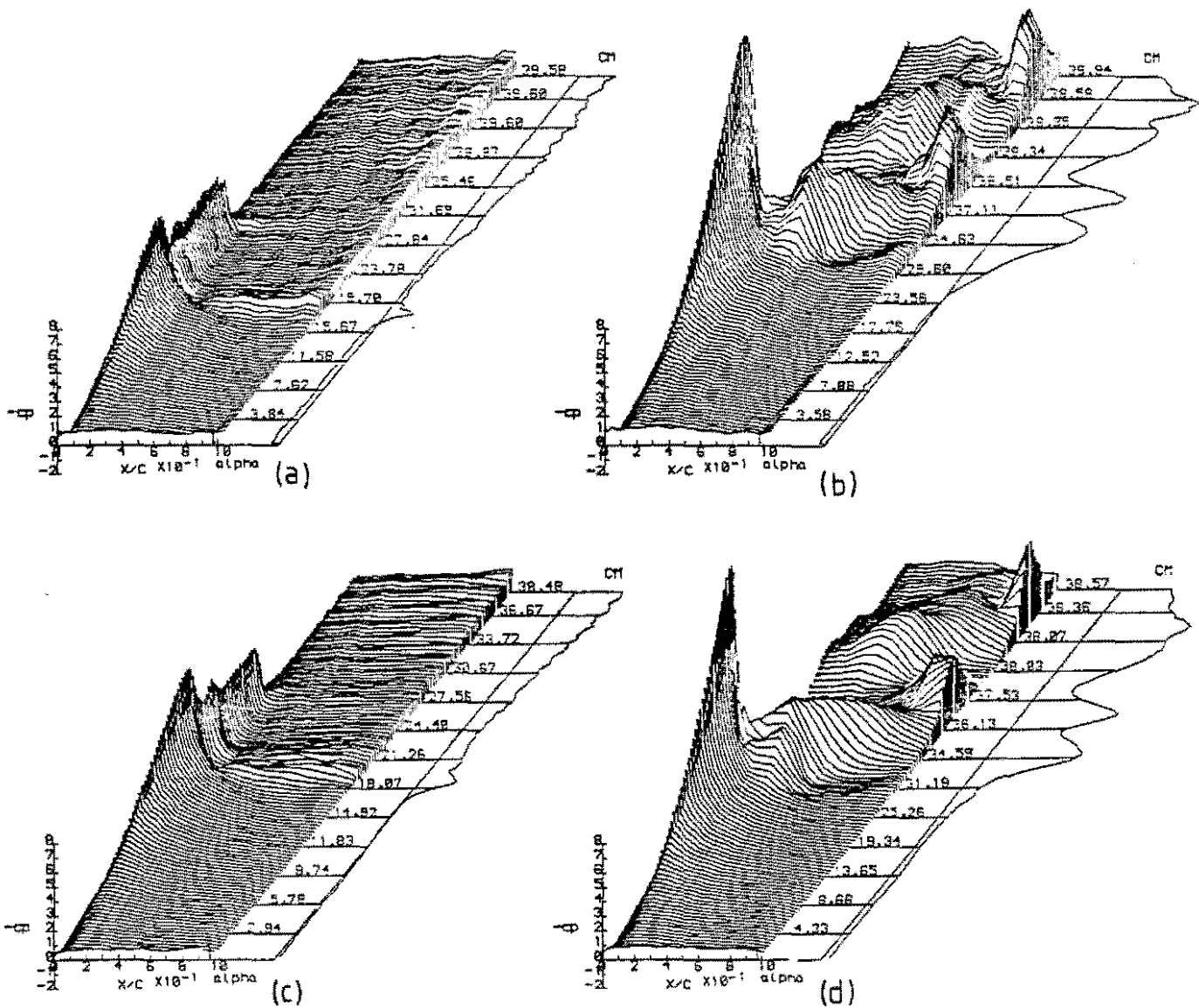


Fig. 8 UPPER SURFACE PRESSURE/TIME HISTORY — RAMP TESTS

Note: (a) $k_1 = 0.004$ } NACA 23012(A) (c) $k_1 = 0.004$ } NACA 23012
 (b) $k_1 = 0.04$ } (d) $k_1 = 0.04$ }

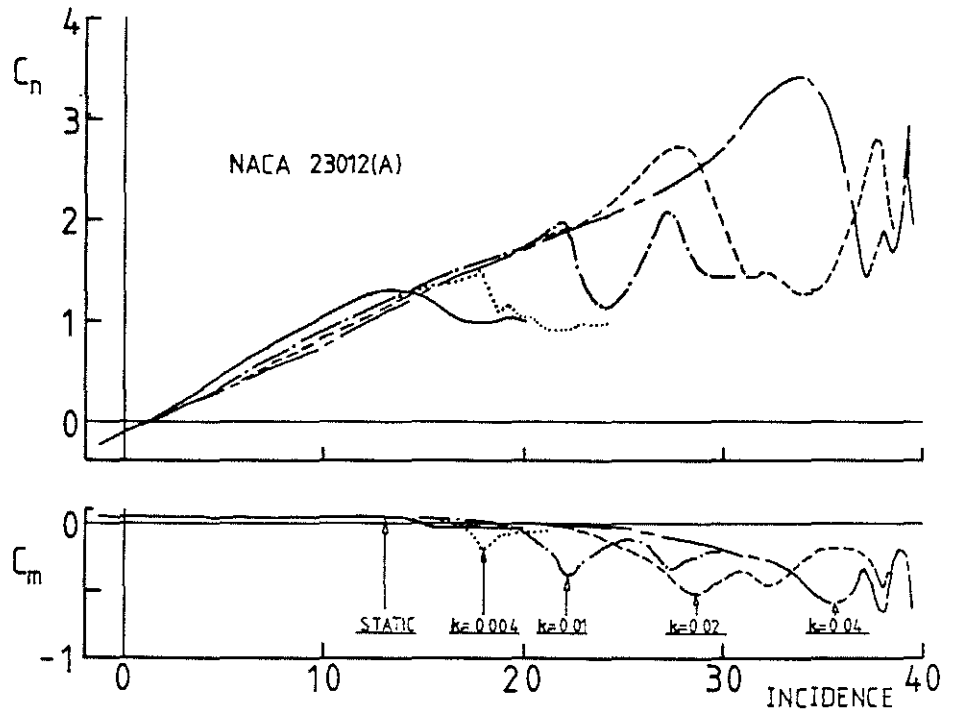


Fig. 9 PERFORMANCE DURING RAMP TESTS
(NACA 23012(A))

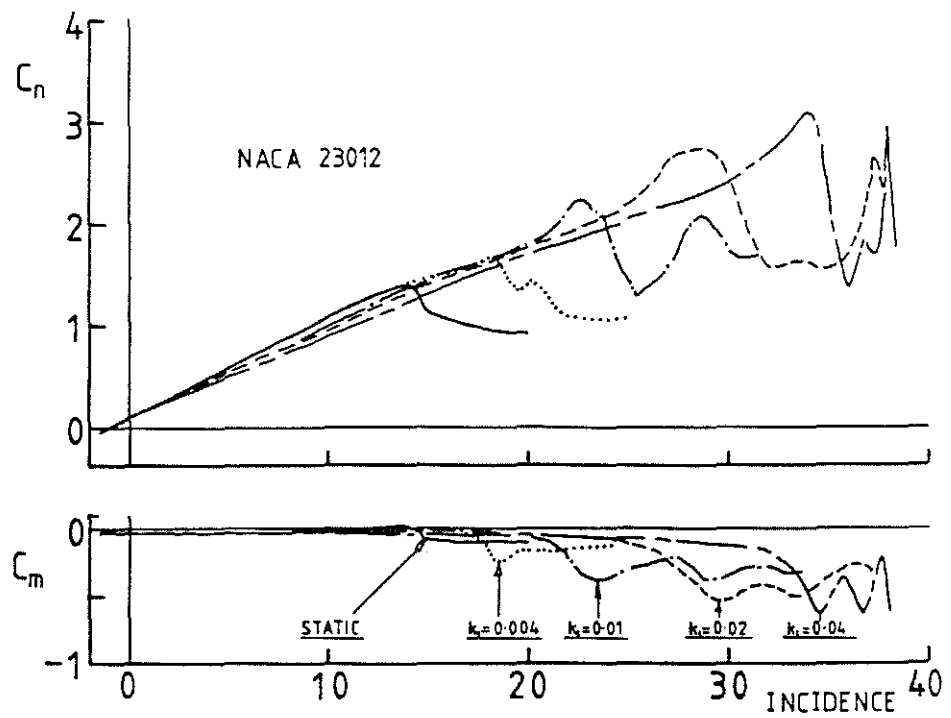


Fig. 10 PERFORMANCE DURING RAMP TESTS
(NACA 23012)

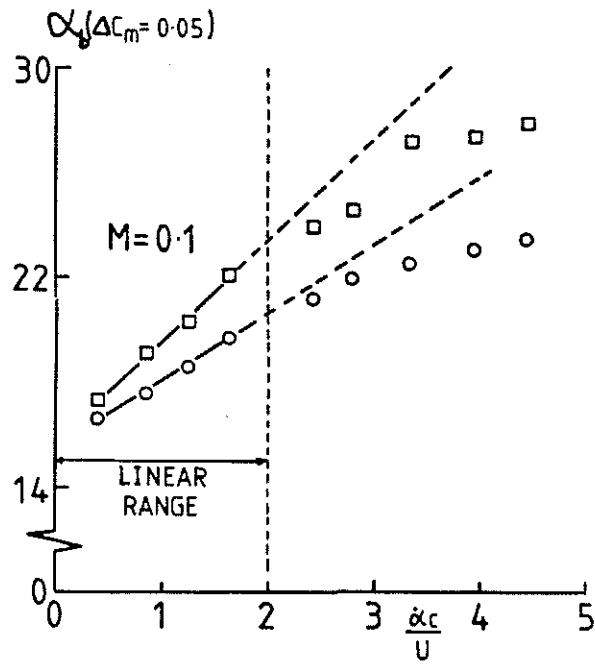


Fig. 11 TIME DELAY CALCULATION - RAMP TESTS

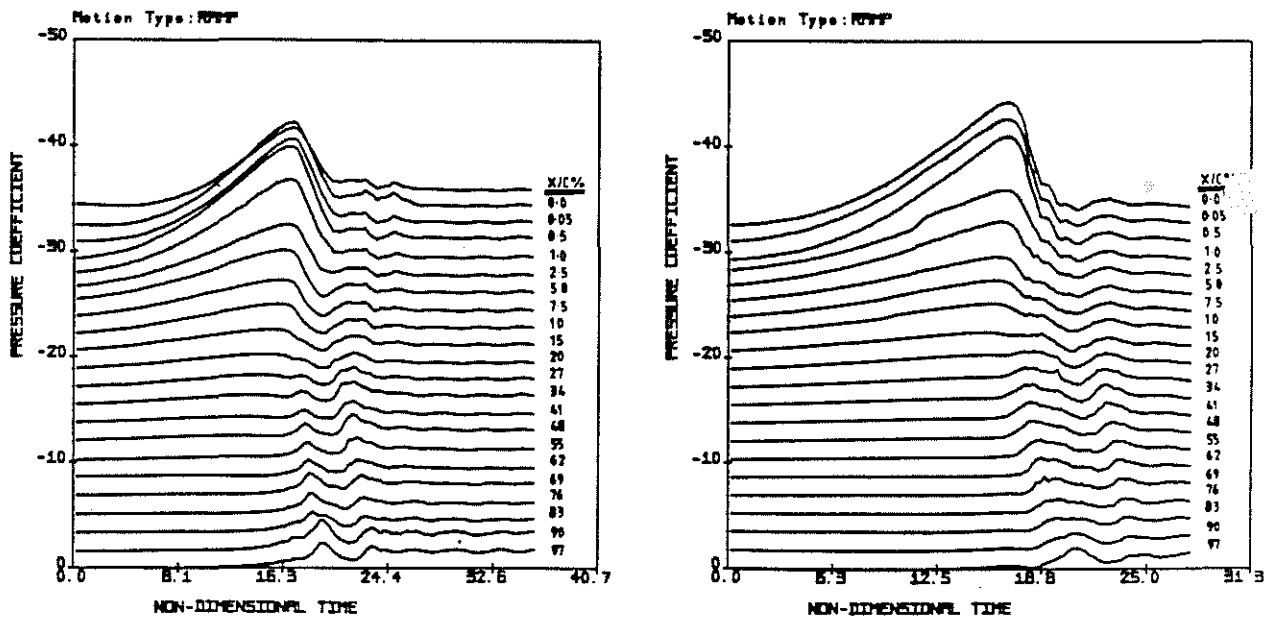


Fig. 12 PSEUDO 3-D PRESSURE HISTORY - UPPER SURFACE